

# Friction Compensation of DC Motors for Precise Motion Control Using Disturbance Observer

M. K .C. Dinesh Chinthaka<sup>1</sup> and A. M. Harsha S. Abeykoon<sup>2</sup>, Non-members

## ABSTRACT

Friction compensation is often neglected in DC servo control systems where precision is not a main concern. However, friction compensation is necessary to achieve precision of a motion control system. In this research work frictional components have been estimated using constant angular velocity motion test and by the use of the disturbance observer. Disturbance observer based friction compensator has been Modeled and developed model was implemented in hardware setup and evaluated using simulation and practical results.

**Keywords:** Disturbance Observer, Friction Compensation

## 1. INTRODUCTION

When developing precise motion control devices, friction plays an important role. Friction is the natural resistance to the movement of a surface with respect to the surface in contact. In order to achieve the best performance, friction compensation methods have been used in many rotary systems. Friction is dependent on the surface of material, characteristics of lubrication and the normal contact force characteristics of the motion control systems [1]. However, it is very hard to obtain exact parametric model for frictional effects, because it's dependent on velocity, system payload, and the system configurations [2]. Therefore several algorithms were developed using standard PID and Artificial Intelligent mechanisms [3]. However such algorithms were not capable of delivering the desired precision under the influence of friction. Static friction, coulomb friction, viscous friction and stribek effect are the available frictional factors in a rotary system [4] while static friction and viscous friction are considered to be linear and other frictional elements are often neglected because either they are insignificantly small or highly nonlinear.

Fuzzy logic [5]-[7], artificial neural networks [8]-[11], neuro-fuzzy [12]-[15], PID based models have been used for friction compensation in most of the

DC servo systems. Friction compensated torque controllers, position controllers or velocity controllers have been developed using artificial intelligent based systems. Researchers haven't estimated the fixed values for frictional effects in most of the cases except in PID based friction compensation systems. It is very important to estimate fixed friction values for a motor because it can be used in any model when developing precise motion control systems. It is not necessary to compensate frictional effects for large scale motors where frictional torques are negligible when compared with the other torques. However it is necessary to compensate friction, in order to achieve high precision of a motion control applications. In this research work authors have proposed a novel concept to compensate friction using disturbance observer (DOB) and reaction torque observer (RTOB). Derived model has further simplified as for the practical use. Frictional elements have been estimated using constant angular velocity motion test and disturbance observer.

## 2. DC MOTOR MODELING

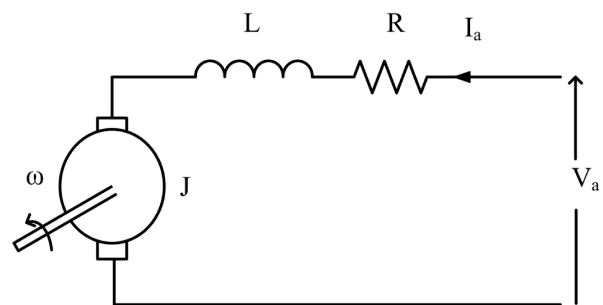


**Fig. 1:** Electrical model of a DC Motor.

DC motors are widely used in numerous control applications, including robot manipulators, disk drives, machine tools and servo actuators and high torque applications etc. DC motor is an essential device in precise motion control applications. DC motor modelling is much simpler with comparing to other motors. DC motor's electrical equivalent model is shown in fig.1. In the fig.1,  $R$  is the armature resistance and  $L$  represents the inductance of the motor [16].

Manuscript received on July 15, 2014 ; revised on January 28, 2015.

Final manuscript received March 23, 2015.

<sup>1,2</sup> The authors are with Department of Electrical Engineering, University of Moratuwa, Sri Lanka, E-mail: dinesh@elect.mrt.ac.lk and harsha@elect.mrt.ac.lk

Supply current is proportional to the motor torque as shown in equation (4). According to the equation (6) generated motor torque is equal to the load torque, motor acceleration, viscous friction and static friction mainly. When motor is not accelerating major fraction of motor torque is consumed by the external load. Static friction is the main frictional element of a motor when comparing to other frictional effects. Viscous friction is always dependent on the rotor angular velocity.

From the Kirchhoff's voltage law following differential equation (1) can be obtained for the DC motor model.

$$V_a = L \frac{dI_a}{dt} + RI_a + E_b \quad (1)$$

If  $E_b$  is the back emf and  $K_e$  is the back emf constant.

$$E_b = K_e \omega(s) \quad (2)$$

From equation (2), Equation (1) can be rewrite as follows in equation (3)

$$V_a = L \frac{dI_a}{dt} + RI_a + K_e \omega(s) \quad (3)$$

If the total mechanical output given by the motor is  $T_m$

$$I_a = \frac{T_m}{k_t} \quad (4)$$

Where  $k_t$  is the torque constant of the motor.

From equation (4), equation (3) can rewrite as in equation (5).

$$V_a = L \frac{d(T_m/K_t)}{dt} + R \frac{T_m}{k_t} + K_e \omega(s) \quad (5)$$

Motor torque  $T_m$  can be written as follows in equation (6).

$$T_m = J \frac{d\omega}{dt} + B\omega + T_{ext} + T_f \quad (6)$$

Where

- $T_f$  : static friction
- $T_{ext}$  : external torque
- $T_m$  : motor torque
- $J$  : inertia constant
- $B$  : viscous friction coefficient
- $\omega$  : angular velocity of the rotor

In  $s$  domain equation (6) and (4) can be represented as follows in (7) and (8).

$$\omega(s) = \frac{T_m(s) - [T_{ext}(s) + T_f(s)]}{Js + B} \quad (7)$$

$$T(s) = k_t I_a(s) \quad (8)$$

As for (7) and (8), DC motor model can be shown as in fig.2, where  $\theta$  is the displacement angle of the rotor and  $T_{int}$  is the interactive torque. For a single motor servo control system interactive torque can be considered as zero. Addition of static friction, viscous friction, load torque, interactive torque is known as the disturbance torque of a motor [17]-[19].

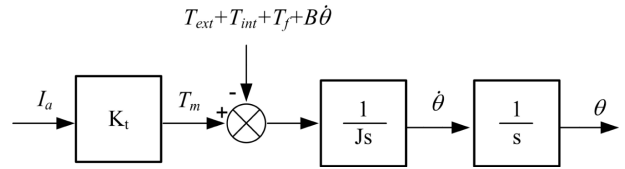


Fig.2: DC motor model.

### 3. MODELING THE DISTURBANCE OBSERVER

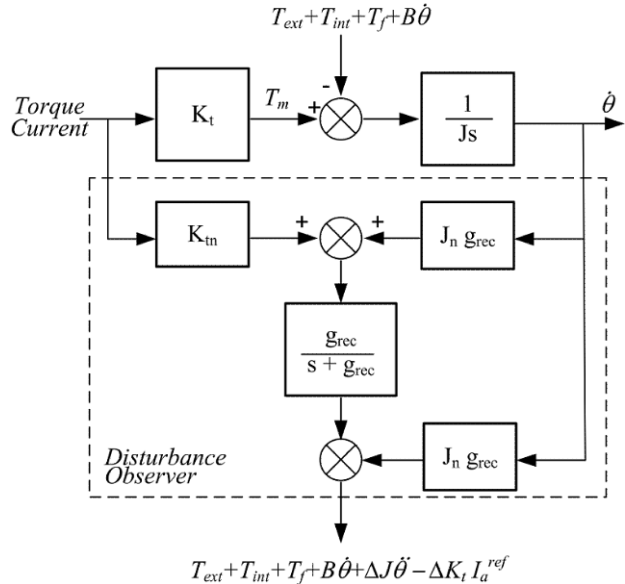


Fig.3: Estimation of Disturbance Torque using DOB.

At the operating conditions load torque motor torque are two torques applied on the electric motor. Load torque could be expressed as in (9).

$$J\ddot{\theta} = T_m - T_l \quad (9)$$

- $T_{dis}$  : disturbance torque
- $T_{int}$  : Interactive torque
- $T_{ext}$  : external torque
- $J_n$  : nominal motor inertia
- $k_{tn}$  : nominal motor constant
- $\Delta J$  : self inertia variation
- $\Delta k_t$  : self motor constant variation
- $\ddot{\theta}$  : rotor acceleration

Load torque can be shown as follows in (10)

$$T_l = T_{int} + T_{ext} + T_f + B\dot{\theta} \quad (10)$$

In (11) and (12) parameters are subjected to change. The total rotor inertia is subjected to change with subsequent modifications of the rotary system.  $k_t$ , motor torque constant may change especially in permanent magnet DC motors when magnetic characteristics deteriorate over the time.

$$J = J_n - \Delta J \quad (11)$$

$$K_t = K_{tn} - \Delta K_t \quad (12)$$

Equation (13) shows the disturbance torque

$$T_{dis} = T_{int} + T_{ext} + T_f + B\dot{\theta} - \Delta J\ddot{\theta} + \Delta K_t I_a^{ref} \quad (13)$$

From equation (10) and (13) the disturbance torque  $T_{dis}$  can be rewritten as,

$$T_{dis} = T_l + \Delta J\ddot{\theta} - \Delta K_t I_a^{ref} \quad (14)$$

From equation (14) and (9),(4)

$$T_{dis} = K I_a^{ref} - J\ddot{\theta} + \Delta J\ddot{\theta} - \Delta K_t I_a^{ref} \quad (15)$$

By substituting terms in equation (11) and (12) in equation (15)

$$T_{dis} = K_{tn} I_a^{ref} - J_n \ddot{\theta} \quad (16)$$

When angular acceleration and motor current are known parameters, it is possible to calculate the disturbance torque ( $T_{dis}$ ) from the block diagram in fig.3. Equation(16) could be represented as shown in fig.3. This implementation is known as the disturbance observer. The low pass filter is included to remove undesirable high frequency responses due to the differentiation stages in the DOB.

#### 4. DOB BASED FRICTION ESTIMATION

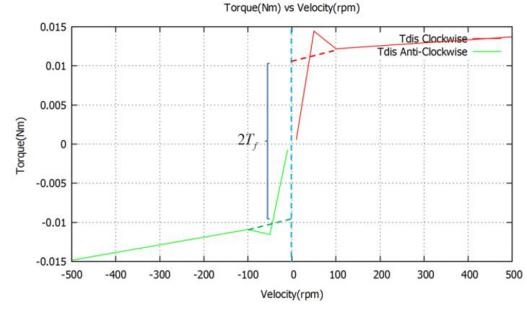


**Fig.4:** Velocity Torque Response of DC motor.

Fig.4 shows the response of constant angular velocity motion test for both clockwise and anticlockwise directions. Disturbance observer is used to estimate the frictional components. When no load is applied, disturbance observer can be used to estimate the frictional elements as shown in (17). Motor was started from standstill to measure the static friction. Here we assume that we have estimated the accurate parameters of  $J$  and  $K_t$  [20]. Therefore,  $\Delta K_t \rightarrow 0$  and  $\Delta J \rightarrow 0$  as explained in (11) and (12).  $T_{int}$  is not present since the apparatus is a single DOF actuator system.  $T_{ext}$  is considered to be zero at no load conditions.

$$T_{dis} = B\dot{\theta} + T_f \quad (17)$$

Initially 0.001A current is commanded to the motor and subsequently, current is increased by the steps of 0.001A. When a motion is detected, the torque output of the disturbance observer was recorded. So this torque is considered to be static frictional torque of that particular direction.

Above test was conducted for velocities in-between -500 rpm to +500 rpm. Viscous friction coefficient could be estimated from the gradient of fig.4.

#### 5. HARDWARE CONFIGURATION

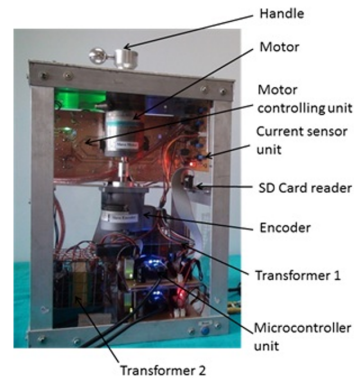


**Fig.5:** Hardware Configuration.

Experimental hardware setup is shown in fig.5. 2500ppr incremental encoder is used for position identification and SD card reader is attached using SPI protocol for data storage. The handle is fixed to the DC motor rotor as shown in fig.6 to provide the external torque.



**Fig.6:** Motor Rotor handle.

## 6. FRICTION COMPENSATION METHODS

### 6.1 Using Disturbance Observer Method (Method A)

Disturbance torque output from the disturbance observer can be shown as in equation (18).

$$T_{dis} = T_{int} + T_{ext} + (J - J_n)\ddot{\theta} + B\dot{\theta} + T_f + (K_m - K_t)I_a^{ref} \quad (18)$$

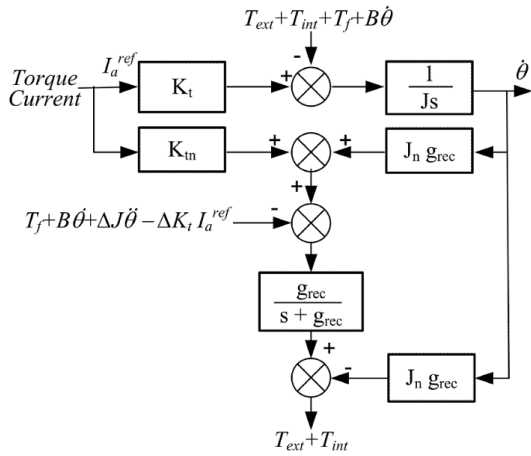
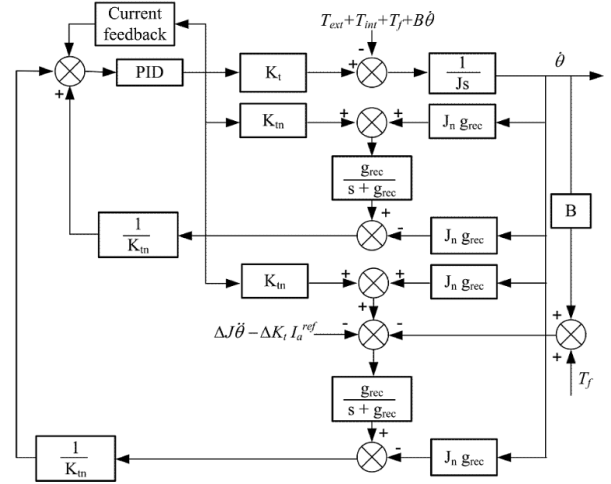


**Fig.7:** Estimation of Reaction Torque using RTOB.

Reaction torque observer has been used for the modeling of friction compensation block diagram too. Frictional effects and changes due to parameter variations are removed from the disturbance observer to compute reaction torque.

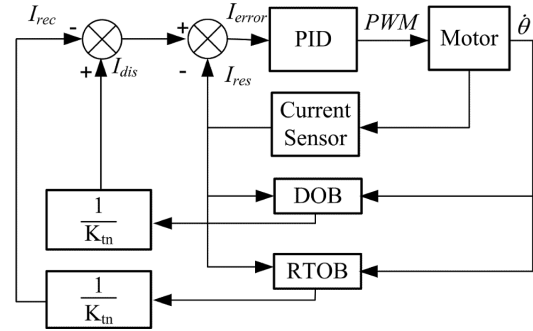
Block diagram of the RTOB is shown in fig.7. For single motor control system  $T_{int}$  can be assumed as zero [20]. External torque could be measured by using the RTOB as shown in fig.7.

Fig .8 shows the modelled block diagram for friction compensation using DOB and RTOB. Estimated values for static friction and viscous friction coefficients from constant angular velocity test can be used



**Fig.8:** Friction Compensator Block Diagram using DOB and RTOB (method A).

in the control block diagram. Changes due to the parameter variation were assumed as zero in practical operating conditions. Block diagram in fig.8 can be shown as in fig.9.



**Fig.9:** Simplified version of DOB and RTOB Friction Compensator.

### 6.2 Simplified and most Effective Block for Friction Compensation (Method B)

Above block diagram illustrate that, actual input from both DOB and RTOB can be shown as follows in fig.10.

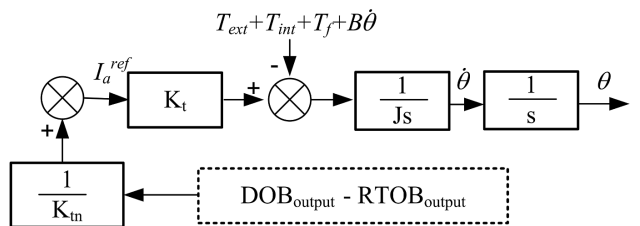


**Fig.10:** Simplified Friction Compensator Block Diagram using DOB and RTOB Methods.

DOB output can be shown as follows in equation (19) and RTOB output as in equation (20)

$$DOB_{output} = (I_a^{ref} K_{tn} + J_n g_{rec} \dot{\theta}) \left( \frac{g_{rec}}{s + g_{rec}} \right) - J_n g_{rec} \dot{\theta} \quad (19)$$

$$RTOB_{output} = [(I_a^{ref} K_{th} + J_n g_{rec} \dot{\theta}) - (B \dot{\theta} + T_f + \Delta J \ddot{\theta} - \Delta K_t I_a^{ref})] \left( \frac{g_{rec}}{s + g_{rec}} \right) - J_n g_{rec} \dot{\theta} \quad (20)$$

Assuming  $\Delta k_t = 0$  and  $\Delta J = 0$  equation (20) can be modified as equation (21)

$$RTOB_{output} = [(I_a^{ref} K_{tn} + J_n g_{rec} \dot{\theta}) - (B \dot{\theta} + T_f)] \left( \frac{g_{rec}}{s + g_{rec}} \right) - J_n g_{rec} \dot{\theta} \quad (21)$$

Using DOB and RTOB equations

$$DOB_{output} - RTOB_{output} = (B \dot{\theta} + T_f) \left( \frac{g_{rec}}{s + g_{rec}} \right) \quad (22)$$

Equation (22) can be demonstrated as shown in fig.12.

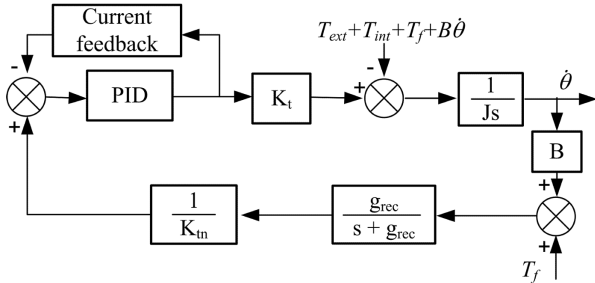


**Fig.11:** Simplified Version of Friction Compensator Block Diagram (method B).

When comparing block diagrams in fig.8 and fig.11, fig.11 contains lesser no of parameters. Method A is bit complicated than method B, therefore algorithm cycle time is much greater in method A. As far as the practical scenario is concerned, method B is the most suitable model for friction compensation purposes.

## 7. STABILITY ANALYSIS

Stability analysis was done for both method A and Method B. Disturbance torque input was considered as the input and angular velocity was considered as the output for analysis. A Matlab algorithm was used for stability analysis. For both models, transfer function was the same as in (23). According to the transfer function, only one pole is at the  $1.396 \times 10^{-21}$ .

If transfer function is G(s)

$$G(s) = \frac{-1.099}{s + 1.396 \times 10^{-21}} \quad (23)$$

Pole is at the left side of the imaginary axis and on the real axis. Therefore both models are stable. DC motor Parameters used for the above analysis are shown in table1. PID gain values of the model was selected using a trial and error method for a PID based current controller. Root locus plot for the both models are shown in fig.12. Fig.13 illustrates the behavior of the system with different inertia values.

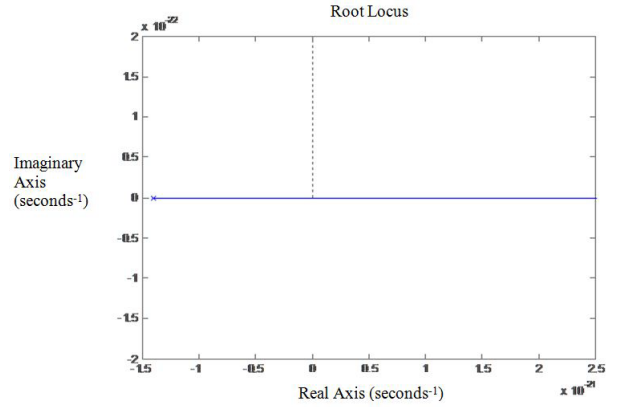


**Fig.12:** Root Locus Plot for the Control Block Diagram.

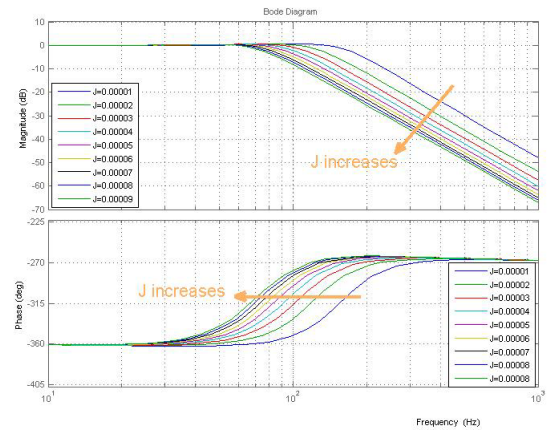


**Fig.13:** Frequency response of the system with different motor inertia values.

## 8. SIMULATION RESULTS

Models in method A and B were implemented in Matlab Simulink. Theoretically, for external torque pulse inputs, if friction is compensated by the derived models, rotor should accelerate for the time interval of the external torque and then it should continuously

**Table 1:** Parameters of the used DC motor.

Parameters	Symbol	Value	Units
Nominal Motor inertia	$J_n$	0.000091	kgm <sup>2</sup>
Motor inertia	$J$	0.000091	kgm <sup>2</sup>
Nominal Torque coefficient	$K_{tn}$	0.134	Nm/A
Torque coefficient	$K_t$	0.134	Nm/A
Proportional constant	$K_p$	0.001	rad/s
Integral constant	$K_i$	0.0001	rad/s
Derivative constant	$K_d$	0.00001	rad/s
Cut-off frequency of low pass filter	$g_{rec}$	200.0	Hz
Viscous friction coefficient	$B$	0.0000021	Nm/rpm
Static friction	$T_f$	0.001119	Nm

rotate at the final velocity. Fig.14 shows the external torque input pulse on the rotor of the Simulink model. Fig.15 shows the output response of the rotor for this external torque pulse input.

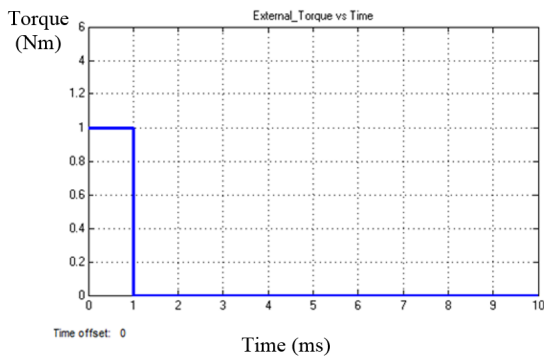
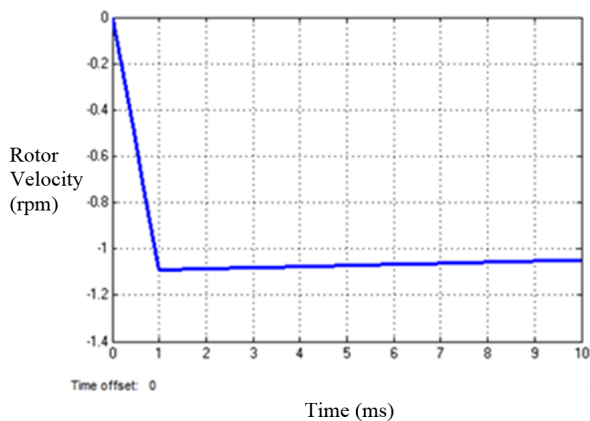
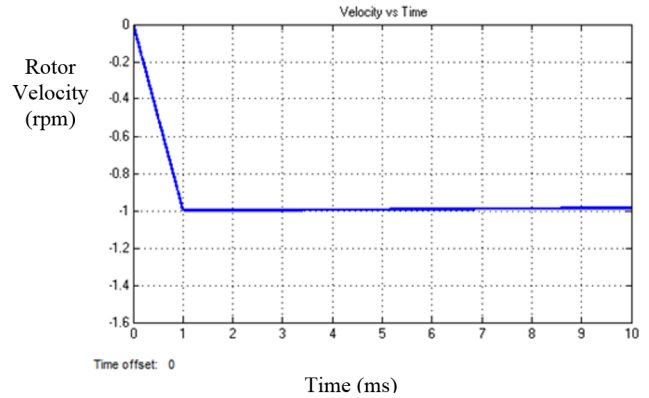
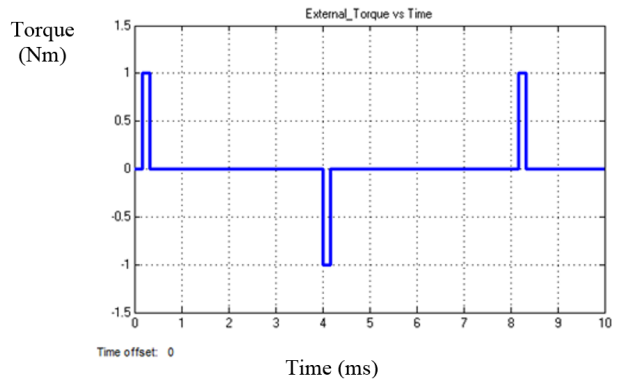
**Fig.14:** External torque variation 1 (A Pulse).

Fig.15 shows the output response without friction compensator. Output response of the motor with the friction compensation is shown in fig.16. Both models show the same output responses in the simulation models.

**Fig.15:** Motor Response 1 (Rotating Speed Variation).**Fig.16:** Motor Response 1 (Rotating Speed Variation).

Then two way external pulses were applied on the rotor as shown in fig.17. Fig.18 shows the output response of the rotor.

**Fig.17:** External Torque variation 2 (Two way Pulses).

For the first torque pulse in fig.17, rotor accelerates for the time of the pulse and continues the rotation from the final velocity obtained. For the second torque pulse, which is equal to the magnitude and opposite in direction, rotor should stop the rotation theoretically as shown in fig.18. This process should repeatedly occur until input torque pulse stops. So both models are theoretically working ideally in the simulation.

## 9. PRACTICAL RESULTS

Models in method A and B was implemented in practical hardware setup and continued the testing procedure. Data was stored in the SD card while doing the testing. Following figures were drawn using Gnuplot. Velocity of the motor should decay in the absence of friction compensation. Fig.19 shows the behavior of the selected DC motor before compensating the friction. External torque pulse was applied by hand and velocity is hardly retained even for two

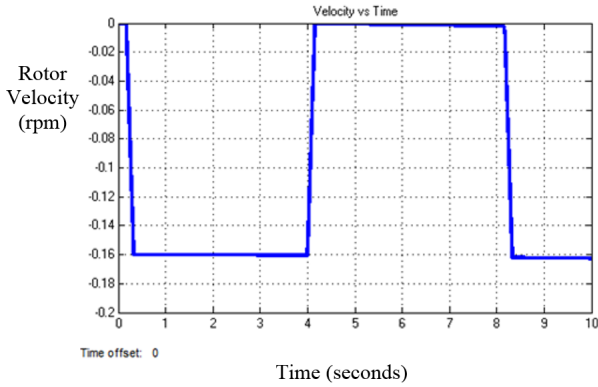


**Fig.18:** Motor Response 2(Rotating Speed Variation).

seconds. It rotates two revolutions without friction compensation.

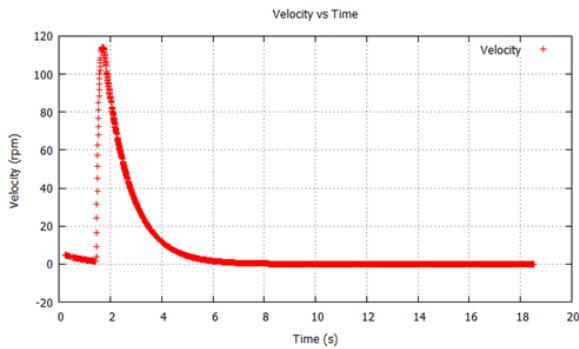


**Fig.19:** Rotor Characteristics without friction Compensator- Single External Torque Pulse.

First, method A was implemented and both static friction and viscous frictions were compensated. Output velocity response for an external torque pulse is shown in fig.20. Velocity retains around 8 seconds but it decays. When the velocity reduces up to certain extent, thereafter velocity decreasing rate goes up.

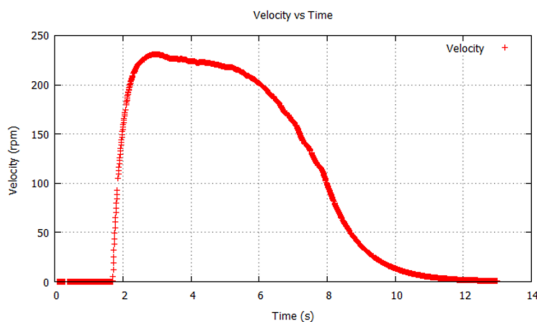


**Fig.20:** Motor Characteristics with method A friction Compensator-Single External Torque Pulse (Both  $F$  and  $B\dot{\theta}$  have been compensated).

Only static friction was compensated using method B model and output response is shown below in fig.21. Velocity decays more rapidly and it is retained around for 10 second.

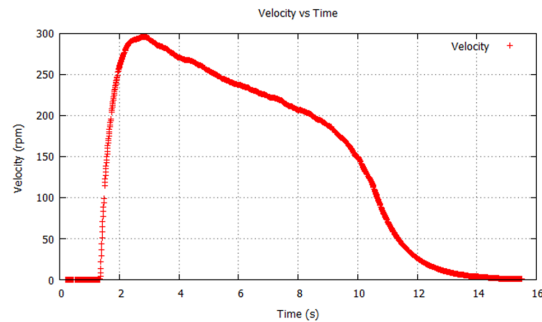


**Fig.21:** Motor Characteristics with friction Compensator-Single External Torque Pulse (Only  $F$  has been compensated).

Then viscous friction is introduced to the compensator. It was rotate almost continuously even for small external torque pulses as shown in fig.22. Even when the speed is as much less as 90 rpm, the system works considerably. The System works for various external torque pulse ranges including very low values.

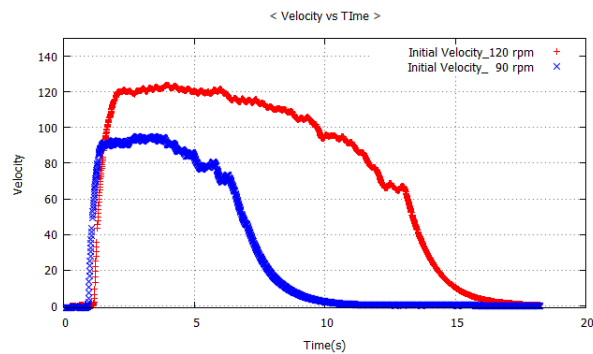


**Fig.22:** Motor Characteristics with friction Compensator-Single External Torque Pulse (For different Velocity Values).

When the initial velocity is higher, velocity is sustained for a longer period as shown in fig.22. Later parts of the decays seem to be identical in shape as in fig.22. This implies that the simple friction model assumed as  $T_f + B\dot{\theta}$  is not fully valid throughout the response. Thus nonlinear effects and/or rotor wide frictional values should be considered for better friction compensation.

Next, continuous external torque pulses were applied for both clockwise and anticlockwise directions. Fig.23 shows the velocity output response of a DC motor without friction compensation. The velocity decays rapidly. When friction compensation is introduced to the system, speed retained much longer until

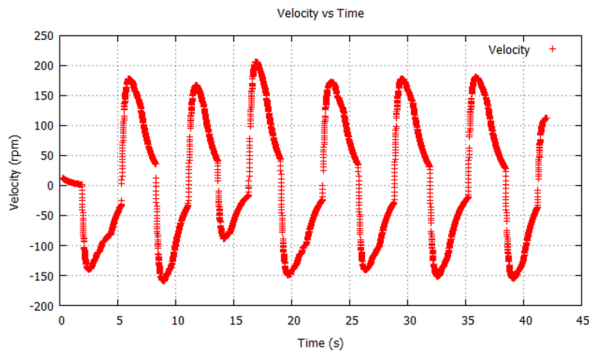


**Fig.23:** Rotor Velocity Characteristics without Friction Compensator-Two way continuous external torque pulse series.

the next torque pulse in the counter direction. Thereafter next counter pulse changes the rotational direction. This process repeatedly occurring until pulse input removes. This result is shown in fig.24.

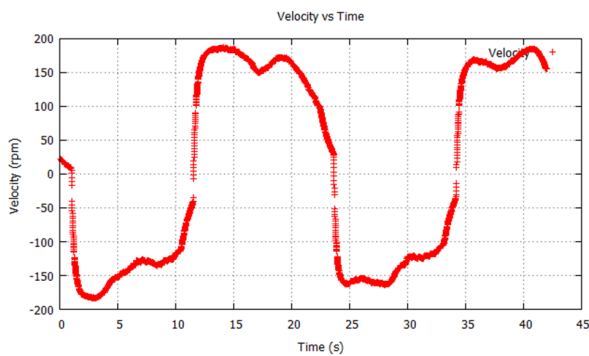


**Fig.24:** Rotor Velocity Characteristics with Friction Compensator-Two way continuous external torque pulse series.

## 10. CONCLUSIONS AND FUTURE WORK

In this research work two models have been proposed for friction compensation. Both methods have been implemented and evaluated using solid simulation and practical results. Both methods produce perfect results in simulations. However as far as practical scenario is concern friction compensation model in method B is more effective. Moreover derived model could be used to verify the static friction value and the viscous friction values which were estimated from the constant angular velocity motion test.

## ACKNOWLEDGEMENT

This "Friction Compensation of DC Motors for Precise Motion Control Using Disturbance Observer" was supported by university of Moratuwa Senate Research Grant Number SRC/LT/2013/12.

## References

- [1] Ruderman, M., "Tracking Control of Motor Drives Using Feedforward Friction Observer," *Industrial Electronics, IEEE Transactions on*, vol.61, no.7, pp.3727-3735, July 2014.
- [2] Mingwei Sun; Zenghui Wang; Yongkun Wang; Zengqiang Chen, "On Low-Velocity Compensation of Brushless DC Servo in the Absence of Friction Model," *Industrial Electronics, IEEE Transactions on*, vol.60, no.9, pp.3897-3905, Sept. 2013.
- [3] Rajasekhar Gundala; Narain, A., "Friction compensation using neural networks applicable to high precision motion control systems in manufacturing," *Industrial Informatics, 2005. INDIN '05. 2005 3rd IEEE International Conference on*, vol., no., pp.808-812, 10-12 Aug. 2005.
- [4] Jing Na; Qiang Chen; Xuemei Ren; Yu Guo, "Adaptive Prescribed Performance Motion Control of Servo Mechanisms with Friction Compensation," *Industrial Electronics, IEEE Transactions on*, vol.61, no.1, pp.486-494, Jan. 2014.
- [5] Donath, H.; Georg, S.; Schulte, H., "Takagi-Sugeno sliding mode observer for friction compensation with application to an inverted pendulum," *Fuzzy Systems (FUZZ), 2013 IEEE International Conference on*, vol., no., pp.1-8, 7-10 July 2013
- [6] Ahmed, M.; Mohd Noor, S.B.B., "Fuzzy control of parabolic antenna with friction compensation," *Intelligent and Advanced Systems (ICIAS), 2014 5th International Conference on*, vol., no., pp.1-4, 3-5 June 2014.
- [7] Tzes, A.; Pei-Yuao Peng; Guthy, J., "Genetic-based fuzzy clustering for DC-motor friction identification and compensation," *Control Systems Technology, IEEE Transactions on*, vol.6, no.4, pp.462-472, Jul 1998.
- [8] Deyin Xia; Liangyong Wang; Tianyou Chai, "Neural-Network-Friction Compensation-Based Energy Swing-Up Control of Pendubot," *Industrial Electronics, IEEE Transactions on*, vol.61, no.3, pp.1411-1423, March 2014.
- [9] Rajasekhar Gundala; Narain, A., "Friction compensation using neural networks applicable to high precision motion control systems in manufacturing," *Industrial Informatics, 2005. INDIN '05. 2005 3rd IEEE International Conference on*, vol., no., pp.808-812, 10-12 Aug. 2005.
- [10] Wahyudi; Tijani, I.B., "Friction compensation for motion control system using multilayer feedforward network," *Information Technology, 2008. ITSIm 2008. International Symposium on*, vol.4, no., pp.1-7, 26-28 Aug. 2008.
- [11] Ciliz, M.K.; Tomizuka, M., "Neural network based friction compensation in motion control," *Electronics Letters*, vol.40, no.12, pp.752-753, 10 June. 2004.

- [12] Daneshwar, M.A; Noh, N.M., "Adaptive neuro-fuzzy inference system identification model for smart control valves with static friction," *Control System, Computing and Engineering (ICC-SCE), 2013 IEEE International Conference on*, vol., no., pp.122-126, Nov. 29 2013-Dec. 1 2013.
- [13] Babaie, M.; Khanzadi, M.R., "Precision motion control for an X-Y table using the LOLIMOT Neuro-Fuzzy Friction compensation," *Robotics and Biomimetics, 2007. ROBIO 2007. IEEE International Conference on*, vol., no., pp.2300-2304, 15-18 Dec. 2007.
- [14] Shiev, K.; Shakev, N.; Topalov, AV.; Ahmed, S., "Trajectory control of manipulators using type-2 fuzzy neural friction and disturbance compensator," *Intelligent Systems (IS), 2012 6th IEEE International Conference*, vol., no., pp.324-329, 6-8 Sept. 2012.
- [15] Hutamarn, S.; Pratumsumwan, P.; Po-ngae, W., "Neuro-Fuzzy based on support vector machine friction compensator in servo hydraulic system," *Industrial Electronics and Applications (ICIEA), 2012 7th IEEE Conference on*, vol., no., pp.2118-2122, 18-20 July 2012.
- [16] Dinesh Chinthaka, M.K.C.; Punchihewa, R.U.G.; Illangarathne, N.C.; Harsha S.Abeykoon, A.M., "Practical Friction Compensation for DC Motors Using the Disturbance Observer," *Artificial Intelligence and Evolutionary Algorithms in Engineering Systems (ICAEES), 2014 International Conference on*, 22-23 April 2014.
- [17] Dinesh Chinthaka, M.K.C.; Punchihewa, R.U.G.; Illangarathne, N.C.; Harsha S.Abeykoon, A.M., "Practical Friction Compensation for DC Motors Using the Disturbance Observer," *Artificial Intelligence and Evolutionary Algorithms in Engineering Systems (ICAEES), 2014 International Conference on*, 22-23 April 2014.
- [18] Sariyildiz, E.; Ohnishi, K., "Adaptive reaction torque/force observer design II," *Industrial Electronics (ISIE), 2014 IEEE 23rd International Symposium on*, vol., no., pp.1168-1173, 1-4 June 2014.
- [19] Dinesh Chinthaka, M.K.C.; Punchihewa, R.U.G.; Harsha S.Abeykoon, A.M., "Disturbance Observer based Friction Compensator for a DC Motor," *Engineering/Electronics, Computer, Telecommunications and Information Technology (ECTI), 2014 International Conference on*, 14-17 May 2014.
- [20] Dayarathna, H.A.N.D.; Prabuddha, L.L.G.; Ariyawansa, K.L.D.N.J.; Chinthaka, M.K.C.D.; Abeykoon, A.M.H.S.; Branesh Pillai, M., "Sensorless contact position estimation of a mobile robot in pushing motion," *Circuits, Power and Computing Technologies*

(ICCPCT), 2013 International Conference on , vol., no., pp.344-349, 20-21 March 2013



**M. K .C. Dinesh Chinthaka** received B.Sc.Eng.Hons degree in Electrical Engineering from University of Moratuwa, Sri Lanka in 2013. He received his M.Sc. in Robotics and Control from University of Moratuwa, Sri Lanka in 2015. His research interests include control systems, industrial automation and robotics, artificial intelligence.



**A. M. Harsha S. Abeykoon** (M'2005 SM'2014) received the B.Sc. degree in Electrical Engineering from University of Moratuwa, Sri Lanka in 2002. He received his M.Sc. and PhD in Robotics and Control from the Keio University, Japan in 2005 and 2008 respectively. From 2009 onwards he has been working in the Department of Electrical Engineering as a Senior Lecturer. His research interests include motion control, mobile robotics and bilateral control related to biomedical engineering. Dr. Harsha is a Senior Member of IEEE and Member of IES. He has worked as the secretary of the IEEE Sri Lanka section. He has received Monbukagakusho scholarship award (from the Japanese Govt.) for 5 years and Keio Leading Lab (KLL) research grant for consecutive 3 years.